



OPTIMIZATION OF A THREE PHASE CONVERTER WITH A HIGH POWER FACTOR UTILIZING IGBTs

José Contreras and Ivo Barbi*

UNIVERSIDAD DE LOS ANDES
Facultad de Ingeniería
Escuela de Ingeniería Eléctrica
Dpto. de Potencia
Tlf. (58) 074-402899
Fax: (58) 074 402890
E-mail josecon@ing.ula.ve
Mérida Edo. Mérida
Venezuela

*FEDERAL UNIVERSITY OF SANTA
CATARINA
Power Electronics Institute – INEP
P.O. Box. 5119 CEP 88-040-970
Tlf.: (55) 482-319204
Fax: (55) 482 34-5422
E-mail ivo@inep.ufsc.br
Florianópolis – SC
Brazil

ABSTRACT:

In this work, the size and weight of a high power factor three-phase converter with soft commutation is optimized with respect to the frequency of operation.

As a work strategy, the losses of the active elements of the converter are calculated (diodes, switches), with the intention of determining the volume of the heat sink, then the Volume vs. Frequency of the passive components (capacitors, inductors and transformers) is determined. The total volume as a function of frequency is presented graphically to determine the minimum volume and the optimum frequency of operation.

Minimizing the size and weight of the converters will allow their use in places with limited spaces like ships, airplanes and so on.

1 INTRODUCTION

Converters with IGBTs that use ZVS/ZCS soft commutation techniques could operate with frequencies as high as

200 Khz, with an efficiency of 90% [1]. Since these high frequencies can be used, the question arises as to which is the optimum frequency that enables minimizing the size and/or the weight of the converter? It could be said that there is a conflict between the reactive components and the heat sink, since the size of the reactive components diminishes with an increase in frequency, but the size of the heat sink increases due to the increment of the commutation losses.

If the reactive components and the heat sink are comparable in size the optimum frequency would be reached and the volume would be minimal [2]. Naturally, this optimum frequency varies with power levels, commutation devices and type of cooling. Therefore, the study could not be exhaustive, but it is possible to determine the optimum frequency for a given number of specifications.

2 CIRCUIT DESCRIPTION

Fig. 1 shows the power circuit for the converter to be analyzed. It consists of a three phase diode rectifier (D1...D6), the main inductors (Lp), the main transformer

(L4, L5), a full-bridge inverter (T1...T4, D7...D10, C1...C4) modulated at constant frequency by phase-shift, an output transformer (L6, L7, L8), an inductor to aid commutation (Lr), a capacitive filter for the bus voltage (C5, C6), an output rectifier (D11, D12), an output filter (Lo, Co) and the load (R)

The primary side of main and the output transformer are connected in parallel, across the point A and B.

The transformation ratio between the main transformer primary and secondary is equal to 2 (two). Thus, the voltage on its secondary (VH2), is equal to $V_c/2$, being V_c the bus voltage CC.

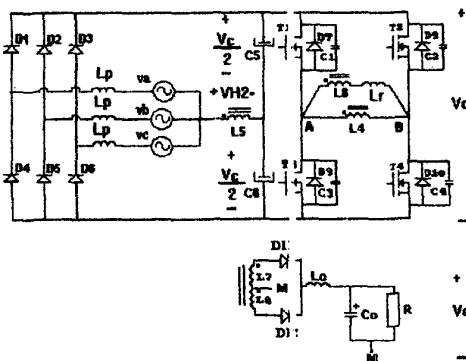


Fig. 1 Power circuit.

The converter main characteristics are: it has only one stage for power processing, which involves the rectifying stage and the power factor correction, soft commutation, operates on fixed frequency, and allows the load galvanic isolation.

The main theoretical waveforms are shown in Fig. 2.

The Fig. 3 shows the theoretical waveforms of the line current and the line to neutral voltage for a low commutation frequency.

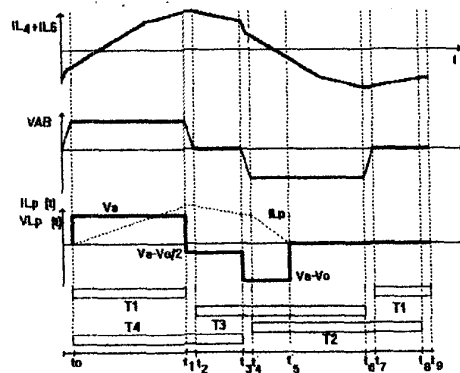


Fig. 2 The main waveforms.

The stages of operation for this circuit are shown in detail in reference [3].

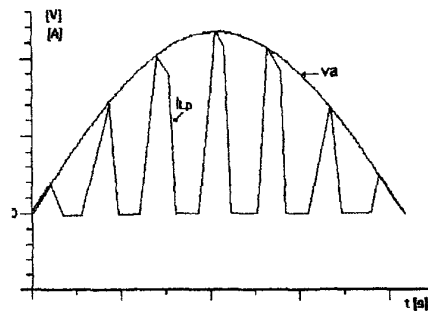


Fig. 3 waveforms of the line current and the line to neutral voltage.

3 WORK STRATEGY

First of all, the losses of the active elements will be calculated (switches) to determine the heat sink volume. Then the volume vs. frequency relationship of the passive components (capacitors, inductor, and transformers) is determined. It is important to rebound who the average current in the rectifier diodes does not depend on the frequency of commutation.

3.1 LOSSES IN THE SWITCHES

The losses in the switches can be divided in two groups: conduction and commutation losses.

3.1.1 CONDUCTION LOSSES

A typical I_{CE}/V_{CE} (current/voltage) curve given by the manufacturer is shown in Fig. 4. This characteristic can be approximated by a straight line (dashed line) which could be calculated by:

$$V_{CE} = I_{med_s} Req + V_{CEO} \quad (1)$$

Where,

$$Req = \frac{V_{CEN} - V_{CEO}}{I_{CN}} \quad (2)$$

V_{CE} = Voltage collector-emitter of the IGBT

V_{CEO} = Voltage threshold of the IGBT

I_{CN} = Reason of I_c

I_c = collector current, and

I_{med_s} = average current in the switch

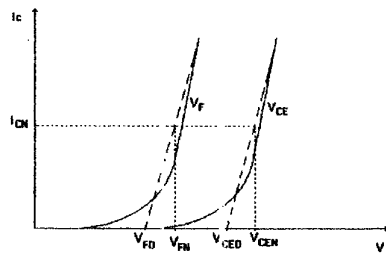


Fig. 4 Voltage vs current in the IGBT and in the diode.

The conduction characteristic of the anti-parallel diode exhibits an exponential behavior, but in the work interval it can be approximated by a straight line with origin at V_{FO} (Fig. 4), this voltage inverse has a typical value of 0,7 volt.

$$V_F = \frac{V_{FN} - V_{FO}}{I_{CN}} I_c + V_{FO} \quad (3)$$

Conduction losses can be calculated as losses in the switch, plus losses in the diode.

Conduction losses in the switch can be calculated by equation (4).

$$P_{con_s} = \frac{V_{CEN} - V_{CEO}}{I_{CN}} (I_{med_s})^2 + V_{CEO} I_{med_s} \quad (4)$$

Losses in the anti-parallel diode can be calculated by equation (5).

$$P_{con_d} = \frac{V_{FN} - V_{FO}}{I_{CN}} (I_{med_d})^2 + V_{FO} I_{med_d} \quad (5)$$

It could easily be shown that the average current in the anti-parallel diode in the switch does not depend on the frequency of commutation, f_s .

3.1.2 COMMUTATION LOSSES

The main commutation losses in the converter under study using IGBTs occur when the switches are turned off, due mainly to the tail current on the IGBT. The losses when the switches are turned on, can be considered negligible.

It can be seen in Fig. 5 that when the switch is turned off the current starts decaying at a fast rate, however, when the current reaches a certain value the decay turns logarithmic (tail current). Energy losses diminishes when a capacitor is placed in parallel with the switch, reducing the voltage stress while the switch is being turned off.

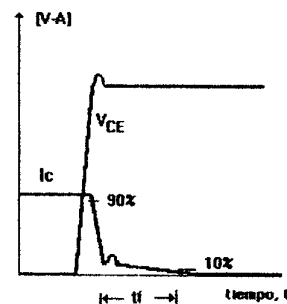


Fig. 5 Voltage and current in the IGBT when the switch is turned off.

Another interesting property of the IGBTs when they are being turned off is

that the tail current occurs under low conditions of dv/dt , particularly at high temperatures. It is evident that the IGBTs behave significantly different for conditions of soft commutation, ZVS, with regard to the conventional conditions of hard commutation, since losses in the turned off region diminish as the capacitor increases, as can be seen Fig. 6. It could also be observed that energy losses increase proportionally to the increment of the turn off current and decrease hyperbolically with the increment of the capacitor [4][5].

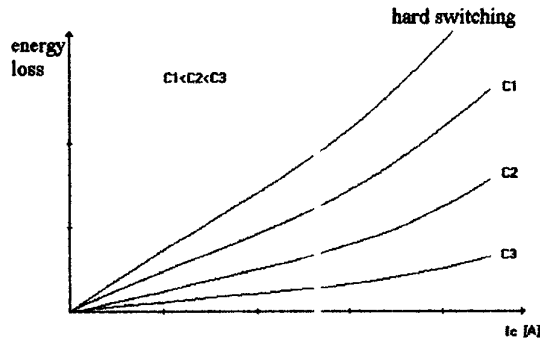


Fig. 6 Losses for several values of turn off current.

Losses during turn off can be calculated approximately by equation (6).

$$E_{off} = \frac{W \cdot (1 + B_T \cdot T) \cdot I_c}{1 + 0,03 \cdot 10^9 \cdot C} \quad (6)$$

Where W and B_T are calculated as follows:

$$W = \frac{E_{off_0}}{I_{c1}} \quad (7)$$

E_{off_0} are the energy losses for $T = 0^\circ C$ and $I_c = I_{c1}$. For $T = T_1$ the losses are E_{off_1} (these values are given by the manufacturer, Fig 7.) Then:

$$B_T = \frac{1}{T_1} \left(\frac{E_{off_1}}{E_{off_0}} - 1 \right) \quad (8)$$

In order to avoid a very large error, for each I_c a new W and B_T should be calculated.

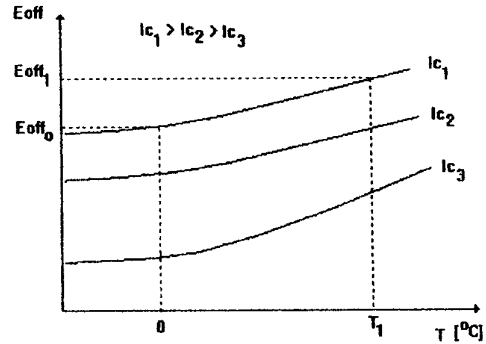


Fig. 7 Energy loss vs. Temperature during turn off.

Finally, total losses in the switch can be calculated by equation (9).

$$P_s = P_{con_s} + P_{con_d} + E_{off} \cdot f_s \quad (9)$$

Fig. 8 shows the switch losses as a function of the frequency of commutation for several values of capacitors. The point of intersection with the abscissa axis ($f_s = 0$) represents the conduction losses for the switch and anti-parallel diode.

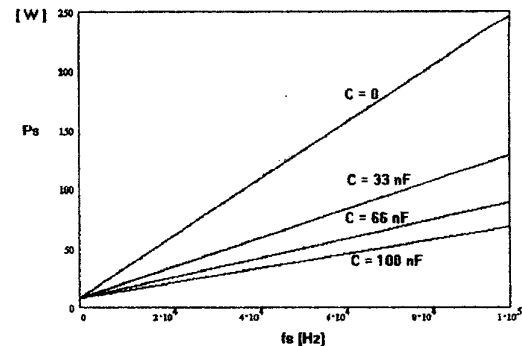


Fig. 8 Switch losses as a function of frequency, for several values of C .

4 CALCULATION OF THE VOLUME OF THE PRINCIPAL TRANSFORMER

The transformer will be dimensioned according to the following expression:

$$A_e \cdot A_w = \frac{VH2 \cdot IL5ef \cdot D_{max} \cdot 10^4}{2 \cdot K_p \cdot K_w \cdot J \cdot B \cdot f_s} \text{ [cm}^4\text{]} \quad (10)$$

Where:

IL5ef is the effective secondary current, A_e is the effective area of the central branch of the nucleus [cm²], A_w is the area of the nucleus window [cm²], K_w is the winding factor, K_p is the primary utilization factor, B is the maximum magnetic flux density [T], f_s is the commutation frequency, D_{max} is the maximum duty cycle rate (0.5), J is the maximum current density [A/cm²] and $VH2$ is the transformer secondary voltage.

$VH2$ can be calculated according to (11).

$$VH2 = \frac{n \cdot V_o}{2} \quad (11)$$

Fig. 9 shows the variation of the product of the areas $A_e \cdot A_w$ as a function of the commutation frequency f_s , for $n=4.8$, $J = 450 \frac{\text{Amp}}{\text{cm}^2}$, and $B = 0.3 \text{ Tesla}$.

The dashed lines indicate commercially available values of type E ferrite nucleus.

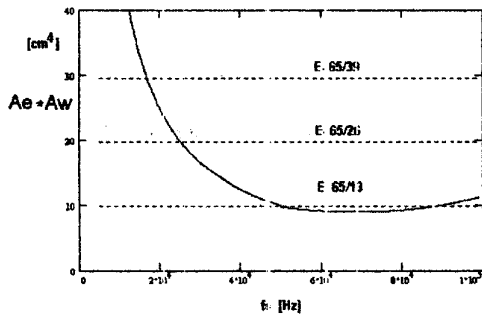


Fig. 9 Area product, $A_e \cdot A_w$, as a function of f_s .

It can be seen in Fig. 9 that $A_e \cdot A_w$, increases abruptly for frequencies lower than 40 Khz. Therefore, the volume of the nucleus also increases. Knowing the value of the product $A_e \cdot A_w$, it is only necessary to

select a nucleus that has an area product equal or greater than the calculated value.

5 CALCULATION OF THE VOLUME OF THE OUTPUT TRANSFORMER

For the output a transformer with a central tap in the secondary is utilized.

$$\text{Taking } P_{O \max} = P_o + 0,1P_o$$

The transformer is dimensioned according to the following expression:

$$A_e \cdot A_w = \frac{P_{O \max} \cdot 10^4}{K_p \cdot K_w \cdot J \cdot B \cdot f_s} \text{ [cm}^4\text{]} \quad (12)$$

Fig. 10 shows the variation of the product of the areas $A_e \cdot A_w$ as a function of the commutation frequency f_s .

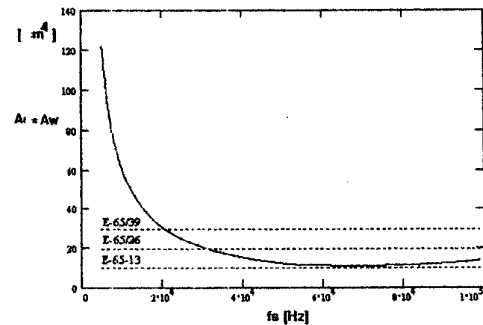


Fig. 10 Area products $A_e \cdot A_w$ as a function of the commutation frequency f_s .

6 POWER INDUCTOR AS A FUNCTION OF FREQUENCY

Fig. 11 shows the inductance of the power inductor as a function of the transformation ratio, between the output transformer primary and secondary, n , for several frequencies of commutation. This inductance is obtained using equation

$$L_p = \frac{3 \cdot V_m^2}{8 \cdot f_s \cdot P_o} I_{p1} \quad (13)$$

The minimum average current in the input rectifier diodes is found for the minimum transformation ratio at which the converter could operate, but the inductance of the main inductor is at a maximum (Fig. 11).

The output transformer should be greater than 3, since a smaller value of n would force the converter to operate in a continuous mode.

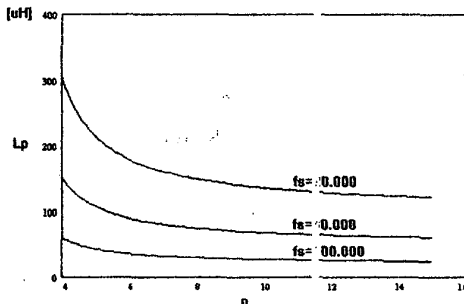


Fig. 11 Inductance of Input inductor as a function of n , for different frequencies of commutation

6.1 VOLUME OF THE POWER INDUCTOR

The product of the areas of an inductor with ferrite nucleus can be defined by the following expression:

$$A_e \cdot A_w = \frac{L_p \cdot I_{pk} \cdot I_{Lrms} \cdot 10^4}{K_{wi} \cdot B \cdot J} \quad (\text{cm}^4) \quad (14)$$

Where: K_{wi} is the winding factor of the inductor (typical value 0,7), The peak current in the inductor can be calculated according to (13).

$$I_{pk} = \frac{V_m \sin(\theta) \cdot D}{f_s L_p} \quad (15)$$

Fig. 12 shows the wave shape of the product of the areas $A_e \cdot A_w$ as a function of the frequency of commutation, f_s , for several values of n .

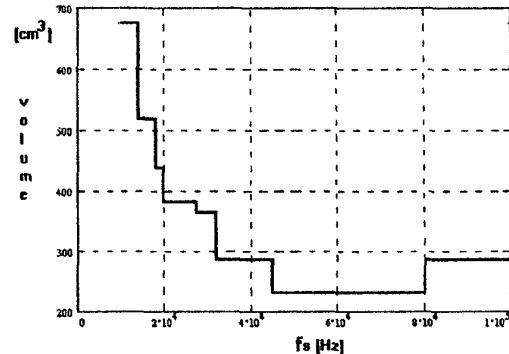


Fig. 12 Product of the areas $A_e \cdot A_w$ as a function of f_s .

Fig. 13 shows the volume of the transformers plus the power inductors, using commercially available nucleus.

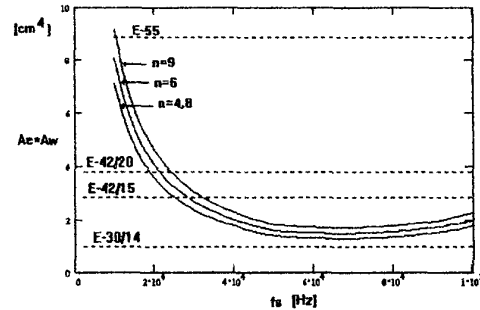


Fig. 13 Volume of the Transformers plus power inductors, using commercially available nucleus.

7 VOLUME OF THE CAPACITORS

Regarding the volume of the capacitors it could be said that their volume is small, having very little effect in the overall volume of the converter. As for the bus capacitors, C_5 and C_6 , these are calculated for a frequency of operation of 360 Hz, therefore present a fix volume that will not be taken into account in the calculation of the total volume of the converter.

8 DETERMINATION OF THE VOLUME OF THE HEAT SINKS

It is assumed that all the IGBTs are mounted on aluminum heat sinks. The value of the thermal resistance between the junction and the capsule, R_{jc} , and the thermal resistance between the capsule and the heat sink, R_{cd} , can be obtained from manufacturer data.

The thermal resistance of the heat sinks could be calculated by equation (16).

$$R_{da} = \frac{T_j - T_a}{P_{diss}} - R_{jc} - R_{cd} \quad (16)$$

Losses in the input and output rectifier diodes do not depend on the frequency of commutation, therefore the heat sinks for the diodes won't be calculated, leaving only the heat sinks for the switches to be calculated.

Placing four switches in a heat sink equation (16) becomes:

$$R_{da} = \left(\frac{T_j - T_a}{P_{con_s} + P_{con_d} + \frac{W \cdot (1 + Bt \cdot T) \cdot I_c}{1 + 0.03 \cdot C} \cdot f_s} - R_{jc} - R_{cd} \right) \cdot \frac{1}{4} \quad (17)$$

Fig. 14 shows the variation of R_{da} , as a function of the frequency of commutation, for several values of C .

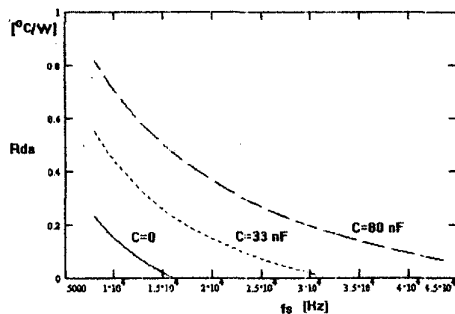


Fig 14 Variation of thermal resistance as a function of the frequency, f_s .

From a SEMIKRON catalog of heat sinks the following data is obtained for a P14 (Fig. 15):

$$w_B = 12 \text{ cm} \quad b = 1 \text{ cm} \quad a = 6 \text{ cm}$$

Where w_B is the width of the heat sink.

For this heat sink in particular, the length could be calculated approximately by equation (18).

$$l = \left[\frac{(13)^{0.6} \cdot 0.7}{R_{sa}} \right]^{\frac{1}{0.6}} \quad (18)$$

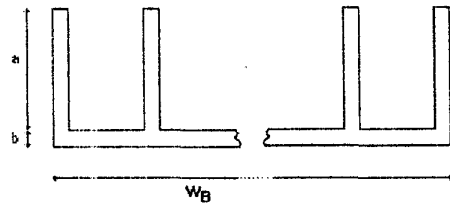


Fig. 15 Heat sink dimensions.

The volume of the heat sink can then be calculated by (19).

$$Vol_{dis} = w_B \cdot (b + a) \cdot l \quad (19)$$

Fig. 16 shows heat sink volume as a function of frequency, for several values of C , taking $T_j = 100 \text{ }^\circ\text{C}$.

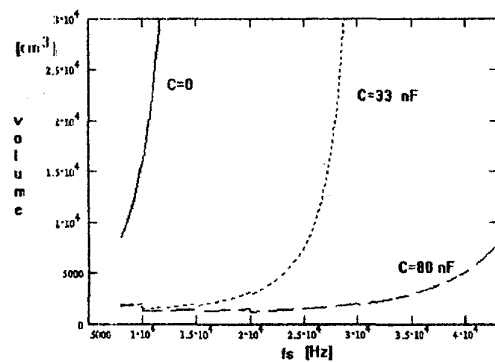


Fig. 16 Heat sink volume as a function of f_s .

As it can be seen from Fig. 16 the minimum volume using hard commutation ($C=0$) is obtained at 10 KHz. As the size of

the capacitor increases, the frequency at which this minimum volume can be obtained increases, locating itself in the range of 10 to 30 KHz.

The next step is to add the volume of the transformers, inductors and heat sinks. Fig. 17 shows this volume for $C = 80 \text{ nF}$ and several values of T_j .

The discontinuities shown in Fig. 17 are due to the fact that commercially available values for the nucleus of the transformers and inductors were used in the calculations. It can be seen that the optimum frequency that allows getting the minimum volume of the converter is in the order of 20 KHz.

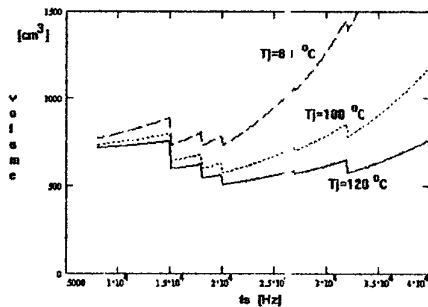


Fig. 17 Volume of the transformers, inductor and the heat sink as a function of f_s .

9 CONCLUSION

It has been shown in this paper that the transformation ratio, n , of the output transformer should be greater than 3, since a smaller value of n would force the converter to operate in a continuous mode, which would bring up as a main disadvantage the presence of high current peaks in the input current.

As the size of the capacitor in parallel to the switch increases the commutation losses are smaller, but it should be kept in mind that the dead time (time available for commutation)

increases, diminishing the maximum duty cycle of operation of the converter.

For the conditions specified for the converter, it was demonstrated that the optimum frequency of operation, that enables getting the minimum volume for the converter, is in the order of 20 KHz.

The utilized procedure could be applied in any other converter.

10 REFERENCES

- [1] Keming Chen and Thomas A. Stuart "A 1.5 KW 200 KHz DC-DC Converter Optimized IGBTs for" High Frequency Power Conversion Conference, Toronto, Canada 1991, pp 265-274.
- [2] Brian J. M., E. William Beans and Thomas A. Stuart "A Study of Volume vs. Frequency for Soft Switching Converters" IEEE PESC'92 Volume I-A pp 625-632.
- [3] José G. Contreras and Ivo Barbi "A Three-Phase High Power Factor PWM-ZVS Power Supply With A Single Power Stage" PESC'94, pp 356-362.
- [4] A. Kurnia, O. Stielau, G. Venkataramanan and D. Divan "Loss Mechanisms in IGBTs Under Zero Voltage Switching" IEEE PESC'92 pp 1011-1017.
- [5] Hans Georg Langer "IGBTs in Full-Bridge DC to DC Converters Comparison of Topologies With Hard and Soft Switching" EPE, 1991, Volume I, pp 562-567.